

Thermodynamically Stable One-Component Metallic Quasicrystals

A. R. Denton* and J. Hafner

Institut für Theoretische Physik, Technische Universität Wien

Wiedner Hauptstraße 8-10, A-1040 Wien, Austria

(January 14, 2022)

Abstract

Classical density-functional theory is employed to study finite-temperature trends in the relative stabilities of one-component quasicrystals interacting via effective metallic pair potentials derived from pseudopotential theory. Comparing the free energies of several periodic crystals and rational approximant models of quasicrystals over a range of pseudopotential parameters, thermodynamically stable quasicrystals are predicted for parameters approaching the limits of mechanical stability of the crystalline structures. The results support and significantly extend conclusions of previous ground-state lattice-sum studies.

PACS numbers: 61.44.+p, 64.70.Dv, 61.25.Mv

Since the landmark discovery [1] of long-range icosahedral quasiperiodic ordering in Al-Mn alloys, quasicrystals have been produced in a rich variety of systems [2,3]. All known quasicrystals, however, are alloys of at least two metallic elements. A fundamental question has therefore naturally arisen: can one-component quasicrystals be thermodynamically stable? A ground-state icosahedral phase has been predicted for an idealized square-well pair potential system [4], although the stability range is confined to a narrow range of well widths and pressures. More recently, extensive lattice-sum potential energy calculations [5] for systems interacting via effective metallic pair potentials have predicted energetically stable ground-state one-component quasicrystals, albeit within a restricted range of pair potential parameters having no counterparts in the Periodic Table. An alternative approach, especially suited to finite temperatures, is classical density-functional (DF) theory [6,7], which determines the free energy of a given solid as the variational minimum with respect to density of an approximate free energy functional. Fundamental applications have already predicted purely entropic hard-sphere quasicrystals to be either metastable [8] or mechanically unstable [9], indicating that ordinary entropy alone is not sufficient to stabilize quasiperiodicity. The question remains whether at finite temperatures longer-range interactions may conspire to stabilize one-component quasicrystals. In this Letter we directly address this question by extending classical DF methods to simple metals interacting via effective pair potentials derived from pseudopotential theory. Taking as a structural model of quasicrystals a certain class of rational approximants, we predict, over a limited range of pseudopotential parameters, thermodynamically stable one-component quasicrystals, stabilized largely by medium- and long-range interactions.

Interactions between ions in a metal are complicated by the presence of conduction electrons and are often best determined by electronic DF methods. However, in cases where the conduction electrons may be considered nearly free, as in the simple metals, it proves possible to replace the strong electron-ion interaction by a much weaker pseudopotential, which is amenable to perturbation theory [10]. The pseudopotential approach [11] essentially reduces the two-component system of electrons and ions to an effective one-component

system of pseudoatoms, interacting via an effective pair potential $\phi(r)$ that depends on the pseudopotential and the density-dependent dielectric function. Here we adopt the popular empty-core pseudopotential [12], parametrized by valence Z and core radius r_c , and the Ichimaru-Utsumi dielectric function [13], which satisfies important self-consistency conditions. For the simple metals, $\phi(r)$ is typically characterised by a steeply repulsive short-range core, a first minimum of varying range and depth, and a relatively weak oscillating tail. Of particular relevance here is that with increasing Z or decreasing r_c the (Friedel) oscillations weaken in amplitude and shorten in wavelength. Correspondingly the core shrinks and, as the oscillations move under the core, a repulsive shoulder may develop.

We now proceed to take $\phi(r)$ as input to a DF theory for a purely classical one-component system of pair-wise interacting pseudoatoms. The DF approach [6,7] defines a functional $F[\rho]$ of the nonuniform one-particle number density $\rho(r)$ that satisfies a variational principle, whereby $F[\rho]$ is minimized (at fixed average density) by the equilibrium $\rho(r)$, its minimum value equaling the Helmholtz free energy. In practice, $F[\rho]$ is separated into an exactly known ideal-gas contribution F_{id} , the free energy of the nonuniform system in the absence of interactions, and an excess contribution F_{ex} , depending entirely upon internal interactions. Note that we ignore here a sizable volume-dependent, but structure-independent, contribution [10], which has no bearing on structural stabilities at fixed average density. The form of $\phi(r)$ for the simple metals naturally suggests decomposition into a short-range reference potential $\phi_0(r)$ and a perturbation potential $\phi_p(r) = \phi(r) - \phi_0(r)$. Such an approach has already been applied with success to Lennard-Jones solids [14,15] as well as to metallic solids [16]. To first order in the perturbation potential [10],

$$F[\rho]' = F_0[\rho] + \frac{1}{2} \int dr \int dr^0 \phi_p(r) \rho(r) \rho(r^0) g_0(r; r^0); \quad (1)$$

where $F_0[\rho]$ is the reference free energy functional and $g_0(r; r^0)$ the reference pair distribution function. Following Weeks, Chandler, and Andersen (WCA) [17], we split $\phi(r)$ at its first minimum and map the steeply repulsive reference system onto a system of hard spheres of effective diameter d , determined at temperature T by the Barker-Henderson prescription [10]

$d = \int_0^{R_1} dr f_1 \exp[-\beta \phi(r) = k_B T \ln g_H S(r)]$. The free energy of the liquid is calculated via the uniform limit of Eq. (1), using the accurate Camahan-Starling $f_{HS}(\rho)$ and Verlet-Weiss $g_{HS}(r)$ [10].

The solid reference free energy is now approximated by the modified weighted-density approximation (MWDA) [18,19], which is known to give an accurate description of the HS system [18]. This maps the excess free energy per particle of the solid onto that of the corresponding uniform fluid f_{HS} , according to

$$F_{ex}^{MWDA}[\rho] = f_{HS}(\hat{\rho}); \quad (2)$$

where the effective (or weighted) density

$$\hat{\rho} = \frac{1}{N} \int d\mathbf{r} \int d\mathbf{r}^0 \rho(\mathbf{r}) \rho(\mathbf{r}^0) w(|\mathbf{r} - \mathbf{r}^0|) \quad (3)$$

is a self-consistently determined weighted average of $\rho(\mathbf{r})$. The weight function $w(r)$ is specified by normalization and by the requirement that $F_{ex}^{MWDA}[\rho]$ generate the exact two-particle (Oststein-Zemike) direct correlation function $c(r)$ in the uniform limit. This leads to an analytic relation [18] between $w(r)$ and the fluid functions f_{HS} and $c(r)$, computed here using the solution of the Percus-Yevick integral equation for hard spheres [10]. The perturbation free energy depends on the pair distribution function of the reference HS solid $g_{HS}(\mathbf{r}; \mathbf{r}^0; d)$, which we approximate in mean-field fashion by the Heaviside unit step function $u(|\mathbf{r} - \mathbf{r}^0| - d)$. This is justified by the fact that in the ordered solid most of the structure of the two-particle density is contained already at the level of the one-particle density, rendering $g_{HS}(\mathbf{r}; \mathbf{r}^0; d)$ a relatively structureless function [19].

Practical calculation of $F[\rho]$ requires specification of the solid structure. Here we consider fcc, hcp, and bcc elementary crystals and a quasicrystalline structure, modelled by a Penrose tiling constructed by projecting a six-dimensional hypercubic lattice onto the three-dimensional physical space. In particular, we consider a hierarchy of rational approximants [2,20] based on the "unit-sphere packing" model of Henley [21]. These are periodic structures obtained by replacing, in the three-dimensional perpendicular space, the golden mean by a rational number $\rho_n = F_{n+1}/F_n$, where F_n is a term in the Fibonacci sequence.

The first four approximants, denoted by 1/1, 2/1, 3/2, and 5/3, have unit cells of 20, 108, 452, and 1904 atoms, respectively, and corresponding maximum HS packing fractions of 0.5020, 0.6400, 0.6323, and 0.6287, compared with 0.6288 in the quasiperiodic limit and 0.7405 for the close-packed fcc and hcp crystals. Also to be specified is the atomic density distribution about the lattice sites of the solid, for which we adopt the widely used Gaussian ansatz. This places at each site R a normalized isotropic Gaussian, such that

$$\rho(r) = \sum_R \frac{1}{\sqrt{3} \pi^{3/2} \sigma^3} \exp\left(-\frac{1}{2} \frac{(r - R)^2}{\sigma^2}\right); \quad (4)$$

where the single parameter σ determines the width of the distribution. The Gaussian ansatz is known [7,22] to reasonably describe the density distribution of close-packed crystals near melting and also should be a good approximation for elastically isotropic quasicrystals.

At fixed T , atomic volume v , Z , and r_c , the free energy is computed from Eqs. (1)–(4) for a given solid structure by minimizing $F[v]$ with respect to v (and the c/a ratio for the hcp crystal). A minimum at $\epsilon = 0$ implies mechanical stability. Finally, comparing free energies of different solid structures and the liquid, the thermodynamically stable structure is determined as that having the lowest free energy. As an essential test of the theory, we have applied it to the HS reference system alone [23]. Briefly, the quasicrystals are predicted to be mechanically stable over a wide range of densities, but always metastable relative to both the liquid and the crystals. Their free energies decrease in order of increasing maximum packing fraction, confirming the decisive importance of packing efficiency in the HS system. Furthermore, their Lindemann ratios (root-mean-square atomic displacement over nearest-neighbour distance) are significantly smaller than those of the crystals, reflecting a higher degree of atomic localization. As a further test of the theory, and of the pseudopotential approach, we have examined the freezing transitions of two simple metallic elements, Mg ($Z = 2$) and Al ($Z = 3$), interacting via effective pair potentials [16]. In both cases, the theory correctly predicts the stable equilibrium structure (hcp for Mg, fcc for Al) and structural energy differences in reasonable agreement with experiment.

We now turn to a broad survey of pseudopotential parameters for the simple metals.

Table I summarizes our results for the thermodynamic state defined by $T = 500K$ and $\rho = 150a_0^{-3}$ (a_0 = Bohr radius) over the ranges $2.0 \leq Z \leq 3.4$ and $0.400 \leq r_c=r_s \leq 0.575$, where $r_s = (3/4\pi Z)^{1/3}$ is the electron-sphere radius. Note that we treat Z here as a continuous parameter to better study trends in relative stabilities. For orientation, we note that near-equilibrium hcp-Mg occurs at $r_c=r_s = 0.501$, while expanded fcc-Al would occur at $r_c=r_s = 0.486$ were it not unstable at such low densities (see below). By default, the liquid is considered the stable phase when the effective HS packing fraction $\phi = \frac{4}{3}\pi r_s^3$ is so low that no solid structure is stable against atomic displacements. At sufficiently high ϕ , where repulsive short-range interactions favour packing efficiency, the close-packed crystals are thermodynamically stable, the minimizing hcp c/a ratio lying close to the ideal ratio $\frac{c}{a} = \sqrt{8/3}$. The more open bcc structure is always at best metastable. Remarkably though, in a narrow band of parameter space corresponding to intermediate ϕ , the quasicrystal structures are predicted to be thermodynamically stable. Although the relevant parameter range contains none of the elements from the Periodic Table, it does include the virtual-crystal parameters (average Z , r_c , and ϕ) characteristic of some of the known multi-component quasicrystals.

We now analyse the physical reasons for quasicrystal stability. When ϕ is so low that the free energy functional has no variational minimum, the solid exhibits a phonon instability. Such unstable regions in the parameter space of Table I can be understood by noting that the effective HS diameter in general decreases with increasing Z (across rows) and with decreasing r_c (down columns). Correspondingly, the solid becomes more loosely packed and the density distributions broader, as reflected by increasing L for a given structure. Ultimately, when $L > 0.10 - 0.15$, the solid loses its stability against vibrational atomic displacements (phonons). As in the HS system, the quasicrystals have consistently smaller L than the crystals, implying greater vibrational stiffness, which tends to enhance their mechanical stability. This partly explains their appearance near the diagonal of Table I, where the crystals lose mechanical stability, as well as the absence of any stable structure towards the lower-right corner. Where no stable structure is indicated, F^* cannot be evaluated within the theory for any of the structures considered. The reason is that at sufficiently

high Z and short r_c , when $\phi(r)$ develops a repulsive shoulder, d may be anomalously large. When d is so large that the maximum $\phi(r)$ for a given structure is exceeded, the repulsive cores of nearest-neighbour atoms overlap at equilibrium separation. This implies a packing instability, which is a second reason for loss of structural stability upon approaching the lower-right corner of Table I. In this parameter region, analysis of structural trends across the Periodic Table [11] and lattice-sum calculations [5] indicate the stability of more open covalent structures, which are, however, outside the scope of the present theory.

Phonon and packing instabilities account for loss of mechanical stability. Insight into the source of thermodynamic stability is gained by examining separate contributions to the total free energy. The reference free energy F_0 combines the entropy and the part of the internal energy associated with short-range interactions, while the perturbation free energy F_p is the remaining part of the internal energy deriving from longer-range interactions. Figure 1 compares F_0 and F_p as a function of Z for the various structures at fixed $r_c=r_s$ and ϕ_0 . As expected, F_0 consistently favours the compact crystals. More revealing is that as Z increases, F_p increasingly favours the more open quasicrystals. This can be understood by noting that with increasing Z , as the Friedel oscillations move under the repulsive core, the first minimum of $\phi(r)$ shifts from the nearest-neighbour distance of the highly-coordinated fcc and hcp structures to shorter distances more commensurate with the lower-coordinated rational approximant structures. Thus the oscillating tail of $\phi(r)$ clearly emerges as the source of thermodynamic stability of simple metallic quasicrystals.

Summarizing, using a practical DF-perturbation theory, we have calculated the free energies of simple metallic one-component crystals and quasicrystals, interacting via effective pair potentials. Separating the full pair potential into a steeply repulsive short-range core and an oscillating tail, the theory minimizes an approximate free energy functional with respect to the density distribution. By surveying a range of pair potential parameters, we have identified general trends in relative stabilities. With increasing valence and decreasing core radius, as the close-packed crystals lose mechanical stability, thermodynamically stable quasicrystals are predicted to emerge. Besides extending to finite temperatures the

intriguing predictions of previous ground-state lattice-sum studies [5], our approach yields new physical insight by linking quasicrystalline stability to enhanced vibrational stiffness and a competition between short- and medium-long-range interactions. Future application to mixtures may help to further explain the stability of real quasicrystalline alloys.

ACKNOWLEDGMENTS

We thank G. Kahl, M. Krajić, and M. Windisch for numerous helpful discussions. This work was supported by the Fonds zur Förderung der wissenschaftlichen Forschung (Austrian Science Foundation) to whom one of us (A.R.D.) is grateful for a Lise-Meitner Fellowship.

* Present address: Institut für Festkörperforschung, Forschungszentrum Jülich GmbH, D-52425 Jülich, Germany (e-mail: a.denton@kfa-juelich.de)

REFERENCES

- [1] Shechtman D., Blech I., Gratias D. and Cahn J.W., Phys. Rev. Lett., 53 (1984) 1951.
- [2] Janot C., Quasicrystals, (Clarendon, Oxford) 1992; Quasicrystals: The State of the Art, edited by Steinhardt P.J. and D'Incenzo D.P., (World Scientific, Singapore) 1991.
- [3] A.P. Tsai, A. Inoue, and T. Masumoto, Jap. J. Appl. Phys. 26, L1505 (1987).
- [4] Narasimhan S. and Jaric M., Phys. Rev. Lett., 62 (1989) 454.
- [5] Smith A.P., Phys. Rev. B, 43 (1991) 11635; Windisch M., Diplomarbeit, (Technische Universität Wien) 1991.
- [6] Oxtoby D.W., in Liquids, Freezing, and Glass Transition, LesHouches session 51, edited by Hansen J.-P., Levesque D. and Zinn-Justin J. (North-Holland, Amsterdam) 1991.
- [7] Lowen H., Phys. Reports 237 (1994) 249; Singh Y., Phys. Reports 207 (1991) 351.
- [8] McCarley J.S. and Ashcroft N.W., Phys. Rev. B, 49 (1994) 15600.
- [9] Popovic M. and Jaric M., Phys. Rev. B, 38 (1988) 808.
- [10] Hansen J.-P. and McDonald I.R., Theory of Simple Liquids, 2nd edition, (Academic, London) 1986.
- [11] Heine V., Solid State Phys. 24 (1970) 1; Hafner J. and Heine V., J. Phys. F: Met. Phys. 13 (1983) 2479; 16 (1986) 1429; Hafner J., From Hamiltonians to Phase Diagrams, (Springer, Berlin) 1987.
- [12] Ashcroft N.W., Phys. Lett. 23 (1966) 48.
- [13] Ichimaru S. and Utsumi K., Phys. Rev. B 24 (1981) 7385.
- [14] Curtin W.A. and Ashcroft N.W., Phys. Rev. Lett. 56 (1986) 2775; 57 (1986) E1192.
- [15] Mederos L., Navascues G. and Tarazona P., Phys. Rev. E 49 (1994) 2161.

- [16] Denton A R., Hafner J. and Kahl G. (unpublished).
- [17] Weeks J D., Chandler D. and Andersen H C., J. Chem. Phys. 54 (1971) 5237.
- [18] Denton A R. and Ashcroft N W., Phys. Rev. A 39 (1989) 4701.
- [19] Curtin W A. and Ashcroft N W., Phys. Rev. A 32 (1985) 2909.
- [20] Goldman A I. and Kelton R F., Rev. Mod. Phys. 65 (1993) 213; Krajić M. and Hafner J., Phys. Rev. B 46 (1992) 10669.
- [21] Henley C L., Phys. Rev. B 34 (1986) 797.
- [22] Young D A. and Alder B J., J. Chem. Phys. 60 (1974) 1254; Ohnesorge R., Lowen H. and Wagner H., Europhys. Lett. 22 (1993) 245.
- [23] Denton A R. and Hafner J., submitted to Phys. Rev. B.

FIGURES

FIG .1. (a) Reference hard-sphere free energy, and (b) perturbation free energy, for designated solid structures, as a function of valence Z at fixed core radius $r_c=r_s = 0.550$, atomic volume $= 150a_0^3$, and temperature $T = 500K$.

TABLES

TABLE I. Thermodynamically stable structure, Lindemann ratio, and effective hard-sphere diameter (in Bohr radii), at fixed atomic volume $v = 150a_0^3$ and temperature $T = 500K$, over a range of valence Z and core radius r_c , as a ratio of electron-sphere radius r_s . (Parentheses indicate metastability with respect to the liquid phase.)

	Z							
$r_c=r_s$	2.0	2.2	2.4	2.6	2.8	3.0	3.2	3.4
0.575	hcp	hcp	fcc	fcc	fcc	5/3	5/3	5/3
	0.0258	0.0285	0.0395	0.0450	0.0507	0.0453	0.0526	0.0631
	5.794	5.692	5.601	5.519	5.445	5.378	5.317	5.262
0.550	hcp	hcp	fcc	fcc	3/2	5/3	5/3	5/3
	0.0315	0.0356	0.0495	0.0554	0.0516	0.0581	0.0690	0.0876
	5.677	5.584	5.501	5.426	5.359	5.299	5.245	5.198
0.525	hcp	fcc	fcc	fcc	5/3	5/3	(5/3)	liquid
	0.0431	0.0558	0.0620	0.0706	0.0653	0.0771	0.0967	{
	5.553	5.470	5.395	5.329	5.271	5.219	5.174	5.135
0.500	hcp	fcc	fcc	(2/1)	(5/3)	(5/3)	liquid	liquid
	0.0625	0.0708	0.0802	0.0789	0.0878	0.109	{	{
	5.422	5.348	5.283	5.228	5.179	5.138	5.104	5.078
0.475	hcp	fcc	(fcc)	(2/1)	(3/2)	liquid	liquid	liquid
	0.0822	0.0931	0.113	0.110	0.135	{	{	{
	5.282	5.219	5.166	5.121	5.085	5.058	5.042	5.042
0.450	(hcp)	(fcc)	(2/1)	liquid	liquid	liquid	{	{
	0.111	0.137	0.134	{	{	{	{	{
	5.136	5.085	5.044	5.013	4.993	4.989	6.964	6.955
0.425	(2/1)	liquid	liquid	liquid	{	{	{	{

	0.131	{	{	{	{	{	{	{
	4.986	4.947	4.920	4.907	6.750	6.785	6.786	6.765
0.400	liquid	liquid	liquid	{	{	{	{	{
	{	{	{	{	{	{	{	{
	4.831	4.806	4.796	6.569	6.619	6.629	6.614	6.584

Fig. 1a (Denton and Hafner)

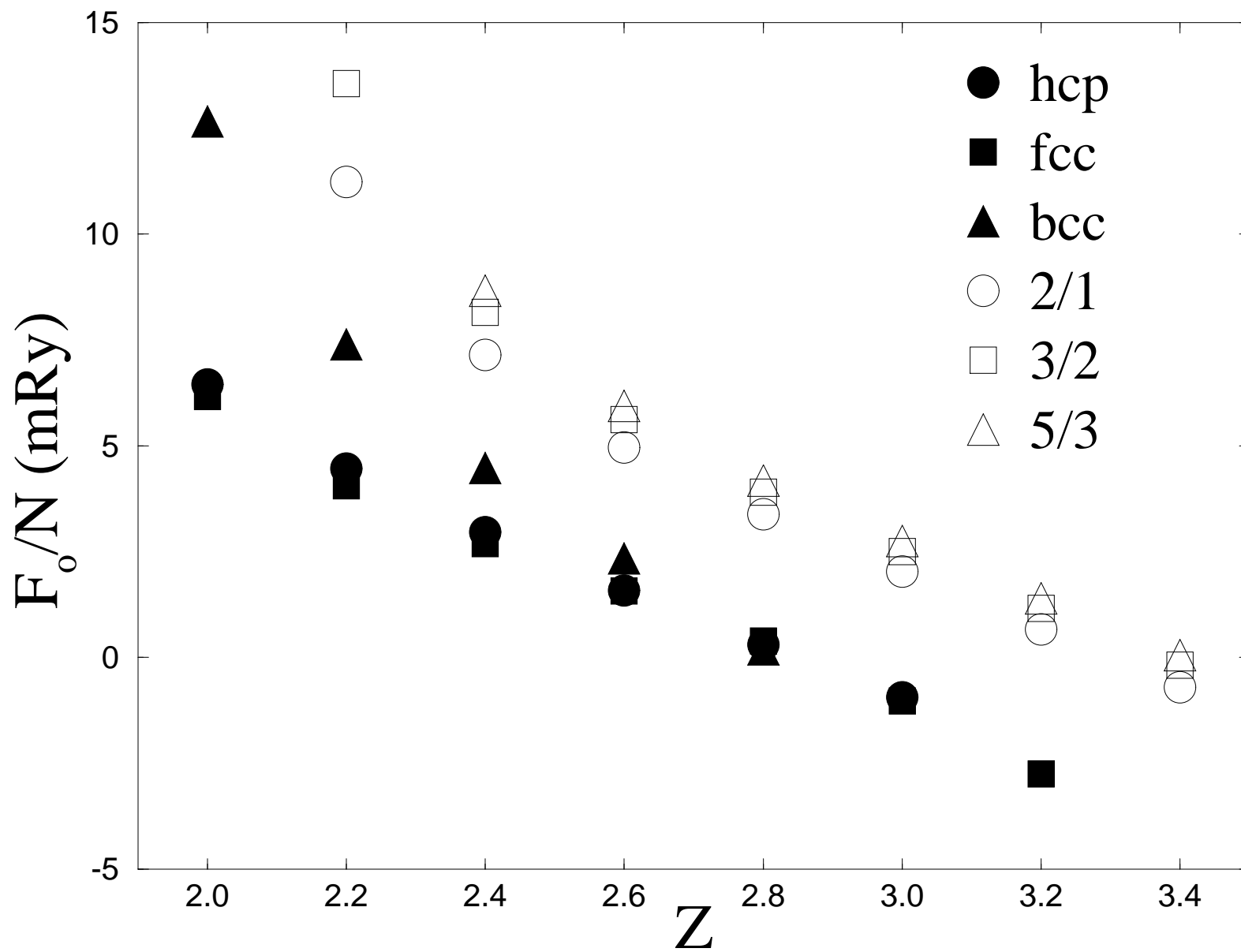


Fig. 1b (Denton and Hafner)

